IDSA · Infectious Diseases Society of America | hivma · hiv medicine association | OXFORD

Human Immunodeficiency Virus-Infected Women Have High Numbers of CD103−CD8+ T Cells Residing Close to the Basal Membrane of the Ectocervical Epithelium

Anna Gibbs,[1] Marcus Buggert,[2,3,4] Gabriella Edfeldt,[1] Petter Ranefall,[5] Andrea Introini,[1] Stanley Cheuk,[1] Elisa Martini,[1] Liv Eidsmo,[1] Terry B. Ball,[6,7] Joshua Kimani,[8] Rupert Kaul,[9] Annika C. Karlsson,[4] Carolina Wählby,[5] Kristina Broliden,[1] and Annelie Tjernlund[1]

[1]Department of Medicine Solna, Center for Molecular Medicine, Karolinska Institutet, Karolinska University Hospital Solna, Stockholm, Sweden; [2]Department of Microbiology and [3]Institute for Immunology, Perelman School of Medicine, University of Pennsylvania, Philadelphia; [4]Department of Medicine Huddinge, Karolinska Institutet, Stockholm, Sweden; [5]Department of Information Technology, Centre for Image Analysis, Uppsala University, Science for Life Laboratory, Sweden; [6]Department of Medical Microbiology, University of Manitoba, Winnipeg, Canada; [7]National Microbiology Laboratory, Public Health Agency of Canada, Winnipeg; [8]Department of Medical Microbiology, Kenyatta National Hospital, University of Nairobi, Kenya; [9]Department of Medicine and Immunology, University of Toronto, Canada

Background. Genital mucosa is the main portal of entry for various incoming pathogens, including human immunodeficiency virus (HIV), hence it is an important site for host immune defenses. Tissue-resident memory T (T_{RM}) cells defend tissue barriers against infections and are characterized by expression of CD103 and CD69. In this study, we describe the composition of CD8+ T_{RM} cells in the ectocervix of healthy and HIV-infected women.

Methods. Study samples were collected from healthy Swedish and Kenyan HIV-infected and uninfected women. Customized computerized image-based in situ analysis was developed to assess the ectocervical biopsies. Genital mucosa and blood samples were assessed by flow cytometry.

Results. Although the ectocervical epithelium of healthy women was populated with bona fide CD8+ T_{RM} cells (CD103+CD69+), women infected with HIV displayed a high frequency of CD103−CD8+ cells residing close to their epithelial basal membrane. Accumulation of CD103−CD8+ cells was associated with chemokine expression in the ectocervix and HIV viral load. CD103+CD8+ and CD103−CD8+ T cells expressed cytotoxic effector molecules in the ectocervical epithelium of healthy and HIV-infected women. In addition, women infected with HIV had decreased frequencies of circulating CD103+CD8+ T cells.

Conclusions. Our data provide insight into the distribution of CD8+ T_{RM} cells in human genital mucosa, a critically important location for immune defense against pathogens, including HIV.

Keywords. CD8+ T_{RM}; genital mucosa; HIV; imaging analysis; in situ.

The mucosal lining of the female genital tract is the main entry portal and initial replication site for various sexually transmitted infections (STIs), including human immunodeficiency virus (HIV), herpes simplex virus (HSV)-2, and human papillomavirus (HPV); thus, study of this lining is critically important to understand robust host immune defenses [1]. In recent studies, a distinct subset of memory T cells, called tissue-resident memory T (T_{RM}) cells, has been described in several tissues, including human female genital tissue [2–5]. After antigen exposure, T cells are recruited to these tissues, where long-lived T_{RM} cells then develop in situ

[6, 7]. Transforming growth factor (TGF)-β and the chemokines CXCL10 (IP-10), CXCL9 (MIG), and CCL5 (RANTES) appear to be crucial for the migration, formation, retention, and functionality of T_{RM} cells [6, 8–10]. Originally, T_{RM} cells were characterized by the surface expression of αE(CD103)β7 integrin together with CD69. CD103 may be important for the retention of T_{RM} cells within the epithelium, through its interaction with E-cadherin, whereas CD69-mediated inhibition of sphingosine-1-phosphate receptor prevents egress of these cells from the tissues [11, 12]. More recently, T_{RM} cells lacking CD103 or CD69 expression have been described in the epithelium and connective tissues [13–16], resulting in a debate about the phenotypic definition of T_{RM} cells.

Vaccine studies have shown that inducing a CD8+ T_{RM} cell response in the genital mucosa is associated with better protection in HSV-2-infected mice [8, 17] and HPV-infected humans [18], suggesting an important role of these cells in controlling persisting genital infections. In this study, we characterized the composition of CD8+ T cells in ectocervical tissues obtained from HIV-infected and uninfected women. Our results contribute to the developing understanding of tissue-resident T-cell identity in genital mucosal tissue and indicate that a relationship exists between HIV and T cell tissue-residency marker expression.

METHODS

Study Populations and Sample Collection and Processing

Swedish Cohort

Cervical mucosa samples were collected from healthy Swedish women (ie, women with good general health and no clinical symptoms of STIs, and those not using any immune suppressive medicine) undergoing hysterectomy for nonmalignant and noninflammatory conditions at the St. Göran Hospital in Stockholm, Sweden (Supplementary Data).

At least 1 cm^3 of mucosa was used for downstream applications. Ectocervical biopsies (8 mm^3), containing both epithelium and underlying subepithelial tissue (ie, submucosa), were dissected from the fresh cervical mucosal samples, snap-frozen, and cryopreserved at −80°C. The remaining tissue specimens were processed into single-cell suspension as previously described [19, 20] (Supplementary Data). Peripheral blood samples were collected from Swedish females undergoing reconstructive skin surgeries [19] who were in the same age range as the women providing cervical tissue samples. Peripheral blood mononuclear cells (PBMCs) were separated by Ficoll-Hypaque density gradient centrifugation and allowed to rest overnight in complete medium before use in flow cytometry experiments. Flow cytometry staining of ectocervical mucosal cells and PMBCs was done as previously described [19] (Supplementary Data).

Kenyan Cohort

Paired peripheral blood samples and 2 ectocervical biopsies were collected from HIV-seropositive (HIV$^+$) female sex workers (FSW), HIV-seronegative (HIV$^-$) FSW, and HIV$^-$ lower risk non-sex working women (HIV$^-$LR). The detailed characteristics of the study population are described in Table 1, Supplementary Data, and previous publications [21–23]. Ectocervical biopsies (3 mm^3) were collected from the superior portion of the ectocervix with Schubert biopsy forceps (B. Braun Aesculap AG, Tuttlingen, Germany) and either placed in a vial containing RNAlater solution (QIAGEN, Valencia, CA) or immediately snap-frozen and cryopreserved at −80°C. Measurement of plasma viral load (VL) and cervical VL of the HIV$^+$FSW individuals have been presented elsewhere [21] (Supplementary Data). The PBMCs were separated by Ficoll-Hypaque density gradient centrifugation and cryopreserved in fetal bovine serum (Life Technologies) containing 10% dimethyl sulfoxide. Procedures for flow cytometry staining of PBMCs were adopted from a previous study [24] (Supplementary Data). All antibodies used for flow cytometry analyses are listed in (Supplementary Table 1a).

Written informed consent was obtained from all study participants, and ethical approval was obtained from the ethics boards at the Kenyatta National Hospital (P53/3/2007), University of Manitoba, and the Regional Ethical Review Board of Stockholm (2007/1036-31, 2013/1377-31/2, 2012/50 31/2).

Table 1. Enrollment Characteristics of the Study Population at Date of Sample Collection

Characteristics	Median or Number (Range or %)						P Value
	HIV$^+$FSW		HIV$^-$FSW		HIV$^-$LR		
	n = 20		n = 18		n = 20		
Age (years)	42	(24–58)	42	(27–51)	38	(24–47)	ns
Plasma VL[a]	16 100	(40–648 000)	n/a		n/a		n/a
Cervical VL[b]	1440	(284–45 800)	n/a		n/a		n/a
Years since HIV diagnosis	3	(1–21)	n/a		n/a		n/a
Bacterial vaginosis	3	(15%)	3	(17%)	3	(15%)	ns
Candida	1	(5%)	2	(11%)	2	(10%)	ns
Chlamydia trachomatis	0	(0%)	0	(0%)	1	(5%)	n/a
Syphilis seropositive	6	(30%)	3	(17%)	1	(5%)	ns
PSA positive[c]	1	(5%)	1	(6%)	1	(5%)	n/a
HSV-2 seropositive	20	(100%)	17	(94%)	9	(45%)	***
Vaginal douching practice							
High[d]	15	(75%)	15	(83%)	6	(30%)	**
Intermediate[e]	5	(25%)	3	(17%)	4	(20%)	ns
Low[f]	0	(0%)	0	(0%)	10	(50%)	***

Abbreviations: CVS, cervicovaginal secretions; FSW, female sex workers; HIV, human immunodeficiency virus; HIV-LR, HIV-lower risk nonsex working women; HSV-2, herpes simplex virus-2; n/a, not applicable; ns, nonsignificant; PSA, prostate-specific antigen; RNA, ribonucleic acid; VL, viral load.

[a]HIV-1 RNA copies/mL plasma.

[b]HIV-1 RNA copies/mL CVS.

[c]PSA detected in CVS >1 ng/mL.

[d]Douching performed >1 time/day with water and soap or water and salt.

[e]Douching performed >1 time/day to 1 time/week with water only.

[f]Douching never performed or <1 time/week with water only.

NOTE: Kruskal-Wallis test followed by Dunn's post hoc test was used for continues variables, and χ^2 test was performed for categorical variables. **, $P < .01$; ***, $P < .001$.

In Situ Staining and Image Analysis

Immunofluorescent staining of the cryopreserved tissue samples was performed as previously described [21]. Immunohistochemistry was performed using the MACH 3 universal HRP Polymer Detection System according to the manufacturer's instructions (HistoLab Products AB, Stockholm, Sweden). The staining reactions were developed with the use of diaminobenzidine tetrahydrochloride (DAB) and Vina Green (HistoLab Products AB). The sections were counterstained with hematoxylin and then mounted with Pertex (Histolab Products AB). The stained tissue sections were scanned into digital images using a Pannoramic 250 Flash Slide Scanner (3DHistech Kft., Budapest, Hungary). Customized computerized image analysis of the immunofluorescent double staining was performed using CellProfiler [25, 26] (Supplementary Data). The triple immunofluorescent and the double immunohistochemistry staining were analyzed by manually counting the positively stained cells within the defined region of interests. Negative controls were incubated with secondary antibody alone. Antibodies used for the in situ staining are listed in Supplementary Table 1b.

Detection and Quantification of Messenger Ribonucleic Acid

Quantification of messenger ribonucleic acid (mRNA) expression in the ectocervical biopsies was performed as previously described [21, 27]. The ABI PRISM 7700 sequence detection system and FAM dye-labeled TaqMan minor groove binder probes and primers (Applied Biosystems, Foster City, CA) were used to quantify the ubiquitin C (UBC), *TGFB1*, *CXCL10*, *CXCL9*, and *CCL5*. Cycle threshold (Ct) values for each target gene were normalized to UBC. Fold change of the target genes was calculated using the 2^{-dCT} equation [28].

Statistical Analyses

Statistical significance of differences between continuous variables was assessed using the Mann-Whitney *U* test for comparisons of independent samples and the Wilcoxon signed-rank test for paired samples. Multiple comparison analysis was performed using the Kruskal-Wallis test followed by Dunn's post hoc test for independent samples. The χ^2 test was performed to assess the statistical significance between categorical variables, and Spearman's rank correlation coefficient test was used to assess correlations. All tests were 2-sided, and a *P* value of <.05 was considered to be significant. The software product used was Prism 5.00 (GraphPad Software Inc, La Jolla, CA) for Windows.

RESULTS

Tissue-Resident CD8+ T Cells in the Healthy Ectocervix Are Located in the Epithelium and Display Cytotoxic Potential

We first characterized the phenotype of tissue-resident CD8$^+$ T cells in the ectocervical mucosa of healthy Swedish women (n = 15, median age 47 [range, 31–51] years). Peripheral blood samples were collected from healthy female volunteers (n = 6,

median age 50 [range, 18–57] years). The ectocervical epithelium was separated from the underlying submucosa, and cell suspensions were analyzed by flow cytometry. Almost all ectocervical CD8$^+$ cells were CD3$^+$ T cells in both epithelial (>99%) and submucosal (>97%) compartments. The majority of these cells displayed an effector memory (EM) phenotype (CD45RA$^-$CD62L$^-$): 84.6% in the epithelium and 64.9% in the submucosa (Supplementary Figure 1). Next, expression of the tissue-resident markers CD69 and CD103 was assessed (Figure 1a), and significantly higher frequencies of CD8$^+$ T cells in the epithelium expressed CD69 (83.7%) and coexpressed CD69 and CD103 (76.0%) than the corresponding submucosal CD8$^+$ T cells (49.0%, *P* = .002 and 18%, *P* < .0001, respectively) (Figure 1b). This indicated a bona fide T$_{RM}$ phenotype (CD45RA$^-$CD62L$^-$ and CD103$^+$CD69$^+$) of epithelial CD8$^+$ T cells. Furthermore, epithelial CD103$^+$CD8$^+$ T cells displayed significantly higher CD103 expression compared with corresponding cells in the submucosa (geometric mean fluorescence intensity [GMFI], 4109 vs 2230; *P* = .03) and compared with blood-derived CD103$^+$CD8$^+$ T cells (GMFI, 4109 vs 2329; *P* = .02) (Figure 1c). In addition, in situ staining of corresponding intact ectocervical tissue confirmed the presence of CD103$^+$ cells within the ectocervical epithelium, where they colocalized with E-cadherin (Figure 1d).

We previously showed that CD103$^+$CD8$^+$ T$_{RM}$ cells within the human cervix display prominent cytolytic potential [19]. We extended these findings by assessing the functional phenotype of CD103$^+$CD8$^+$ and CD103$^-$CD8$^+$ T$_{RM}$ cells. First, CD8$^+$ T cells (TCRγδ$^-$CD3$^+$CD8$^+$) accounted for most of the production of total granzyme (Gzm) B (89.0%) and perforin (94.8%) in the ectocervical epithelium (Supplementary Figure 2a). Second, no differences were observed between CD103$^+$CD69$^+$CD8$^+$ and CD103$^-$CD69$^+$CD8$^+$ T$_{RM}$ cells, with respect to steady-state expression of GzmA (67.2% vs 80.1%), GzmB (42.4% vs 31.2%), and perforin (61.3% vs 66.5%). Furthermore, there was almost no active production of interferon (IFN)-γ in the 2 subpopulations of CD8$^+$ T$_{RM}$ cells (0.05% vs 0%) in steady-state conditions (Supplementary Figure 2b).

The Ectocervical Epithelium of Human Immunodeficiency Virus-Infected Women Contains Elevated Frequencies of CD103–CD8+ Cells

We previously showed that women infected with HIV displayed elevated frequencies of CD8$^+$ cells in their ectocervical epithelium [21]. In this study, we further characterized the tissue-resident phenotype of these epithelial CD8$^+$ cells in HIV$^+$FSW, HIV$^-$FSW, and HIV$^-$LR groups. In situ staining for CD8 and CD103 (Figure 2a) was assessed by computerized image-based in situ analysis (Supplementary Data). The numbers of epithelial CD103$^+$CD8$^+$ cells/mm^2 were comparable between the groups (284 vs 386 and 293; *P* = .76); however, the HIV$^+$FSW group displayed significantly higher numbers of epithelial CD103$^-$CD8$^+$ cells/mm^2 and proportion of CD103$^-$CD8$^+$ cells among total CD8$^+$ cells than the
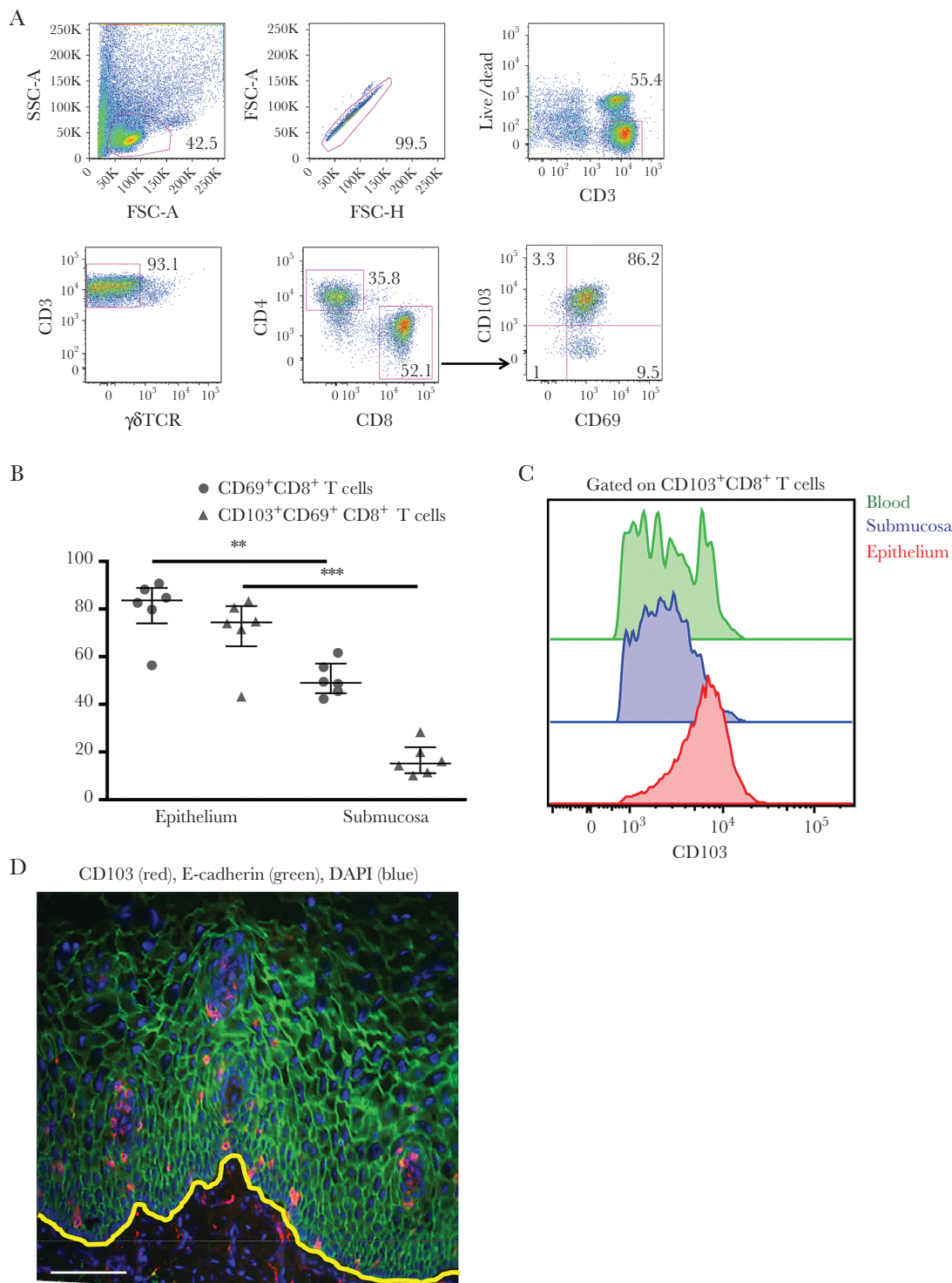
Figure 1. Characterization of tissue-resident CD8+ T cells in ectocervical tissues obtained from the healthy Swedish women (n = 6). (a) Representative plot showing the gating strategy for tissue-resident CD8+ T cells (eg, CD69+CD103+CD8+ T cells). (b) Scatter plot showing frequencies of CD69+CD8+ T cells and CD103+CD69+CD8+ T cells within total CD8+ T cells from epithelium and submucosa. One of the 3 HPV deoxyribonucleic acid-positive donors expressed low levels of CD69 and CD103 on the ectocervical epithelial CD8+ T cells and was considered an outlier. Each point represents a different subject: CD69+CD8+ T cells (circle) and CD103+CD69+CD8+ T cells (triangle). Horizontal lines represent median ± interquartile range. Statistical significance was determined using the Wilcoxon signed-rank test; **, $P < .01$ and ***, $P < .001$. (c) A representative histogram showing expression levels of CD103 on CD103+CD8+ T cells obtained from the ectocervical epithelium (red), ectocervical submucosa (blue), and blood (green). (d) A representative immunofluorescence image of an ectocervical tissue section stained for CD103 (red) and E-cadherin (green). 4′,6-Diamidino-2-phenylindole ([DAPI] blue) was used as a counterstain for visualization of cell nuclei. The yellow line indicates the basal membrane, which separates the epithelium from the underlying submucosa. The image was collected with ×20 objective, and the scale bar represents 100 µm. Abbreviations: FSC-A, forward scatter area; FSC-H, forward scatter height; SSC-A, side scatter area; TCR, T-cell receptor.

HIV⁻FSW and HIV⁻LR groups (275 vs 133 and 138, $P = .0001$ and 50% vs 29% and 30%, $P = .0004$, respectively) (Figure 2b).

Furthermore, the CD103⁻CD8⁺ cells localized significantly closer to the basal membrane of the ectocervical epithelium than the CD103⁺CD8⁺ cells, in all 3 groups (HIV⁺FSW: 14 vs 33 µm, $P = .0009$; HIV⁻FSW: 15 vs 36 µm, $P = .002$; and HIV⁻LR: 15 vs 24 µm, $P = .006$) (Figure 2c). Within the HIV⁺FSW group, the number of epithelial CD103⁻CD8⁺ cells, but not number of CD103⁺CD8⁺ cells, correlated significantly with women's cervical and plasma VL (Figure 2d and data not shown).

Next, expression of early proliferation marker Ki67 was assessed on CD103⁺ and CD8⁺ cells. Ki67⁺ cells were seen in the basal and parabasal epithelial cell layers. Neither CD103⁺ cells nor CD8⁺ cells coexpressed Ki67 within the ectocervical epithelium in any of the groups (Supplementary Figure 3a). CD69 expression was assessed on epithelial CD103⁺CD8⁺ and CD103⁻CD8⁺ cells to define the tissue-resident phenotype of these cells (Supplementary Figure 3b). Approximately all epithelial CD8⁺ cells expressed CD69 in all groups (HIV⁺FSW, 98.2%; HIV⁻FSW, 99.3%; and HIV⁻LR, 97.8%) (data not shown), suggesting that both CD8⁺CD103⁺ and CD8⁺CD103⁻ cells in the ectocervical epithelium are T_{RM} cells.

Ectocervical Biopsies of Human Immunodeficiency Virus-Infected Women Contain Elevated Levels of Chemokine Messenger Ribonucleic Acid

Transforming growth factor-β is important for upregulation of CD103 and for the formation of T_{RM} cells [6, 9], whereas the CXCL10, CXCL9, and CCL5 chemokines are crucial for the recruitment of circulating memory T cells to vaginal tissue in mice [8, 10]. Therefore, the mRNA levels of *TGFB1*, *CXCL10*, *CXCL9*, and *CCL5* were assessed in the ectocervical tissues obtained from the Kenyan women. Significant differences were seen between the study groups in respect to mRNA expression of *TGFB1* ($P = .0009$), *CXCL10* ($P = .006$), *CXCL9* ($P = .001$), and *CCL5* ($P = .0001$), and the HIV⁺FSW group displayed the elevated levels of all genes assessed compared with the control groups (Figure 3a). Thereafter, the chemokine expression was correlated with the number of CD8⁺ cells in the ectocervical epithelium of HIV⁺FSW group. We found no correlation between chemokine mRNA expression and the number of epithelial CD103⁺CD8⁺ cells (data not shown). However, significant positive correlations between mRNA expression of *CXCL10*, *CCL5*, and a positive trend of *CXCL9*, and the number of epithelial CD103⁻CD8⁺ cells were found. No correlation was found between CD103⁻CD8⁺ T cells and *TGFB1* mRNA expression (Figure 3b). In addition, *CXCL9* and *CCL5* mRNA expression correlated significantly with plasma VL, whereas *CXCL10* correlated significantly with both plasma and cervical VL (Figure 3c and d).

Both CD103+ Cells and CD103– Cells Within the Ectocervical Epithelium Express Cytolytic Molecules

We next investigated whether CD8⁺ T cells from the ectocervical epithelium of women infected with HIV have altered effector potential compared with the control groups. No statistical difference was observed among the percentage of GzmA⁺CD8⁺, GzmB⁺CD8⁺, and perforin⁺CD8⁺ cells within the total CD8⁺ cells in the 3 study groups (HIV⁺FSW: 25.5%, 6.3%, and 2.2%, HIV⁻FSW: 17.2%, 1.5%, and 2.4%, and HIV⁻LR: 19.4%, 3.4%, and 1.5%, respectively) (Figure 4a and b). In addition, the frequency of IFN-γ⁺CD8⁺ cells was close to null in all study groups (HIV⁺FSW, 0.5%; HIV⁻FSW, 0%; and HIV⁻LR, 0%) (data not shown). It is of interest to note that although GzmA⁺, GzmB⁺, and perforin⁺ cells were present in both the epithelium and submucosa, IFN-γ⁺ cells were mainly present in the submucosa (Figure 4a) (data not shown).

Expression of the cytolytic molecules, GzmA, and perforin in combination with CD103 was also assessed. Epithelial CD103⁺ cells expressed GzmA and perforin; however, single-positive GzmA and perforin cells were also seen in 3 study groups (Figure 4c and data not shown).

Human Immunodeficiency Virus-Infected Women Have an Altered CD103 Expression on Circulating CD8+ T Cells

We further investigated whether an altered CD103 expression, as seen on CD8⁺ cells in the ectocervix of women infected with HIV, could also be observed in their blood. Hence, the phenotype of circulating CD8⁺ T-cell expressing CD103 was investigated with use of flow cytometry (Figure 5a). We observed that the HIV⁺FSW group displayed a significantly lower percentage of circulating CD103⁺CD8⁺ T cells among total CD8⁺ T cells than the HIV⁻FSW and the HIV⁻LR groups (0.9% vs 2.4% and 3.0%, respectively, $P < .0001$) (Figure 5b). Furthermore, a positive trend, although not significant, was observed between the percentage of circulating CD103⁺CD8⁺ T cells and the percentage of CD103⁺CD8⁺ from the ectocervical epithelium of the HIV⁺FSW group (r = 0.45, $P = .08$) (data not shown). In addition, we found significantly higher frequencies of circulating CD103⁺CD8⁺ T cells expressing activation markers CD38 and HLA-DR in the HIV⁺FSW group (27.6%) than the HIV⁻FSW (5.0%) and the HIV⁻LR (4.3%, $P < .0001$) groups (Figure 5c). Although no significant difference was seen between the frequencies of CD103⁺CD8⁺ T cells expressing the inhibitory receptor PD-1 (associated with T-cell exhaustion in individuals infected with HIV) [29, 30] among the HIV⁺FSW (41.6%), the HIV⁻FSW (35.1%), and the HIV⁻LR (32.2%, $P = .1$) groups, PD-1 expression on CD103⁺CD8⁺ T cells was elevated in the HIV⁺FSW group ([GMFI] HIV⁺FSW: 786, HIV⁻FSW: 693, and HIV⁻LR: 746; $P = .04$) (Figure 5d and e). Frequencies of both circulating CD38⁺HLA-DR⁺CD103⁺CD8⁺ T cells and PD-1⁺CD103⁺CD8⁺ T cells in HIV⁺FSW correlated significantly with their plasma VL (Figure 5f).

Finally, in all study groups, circulating CD103⁺CD8⁺ T cells consisted of several memory subsets, with a negligible frequency of naive and central memory cells and high frequency of transitional memory (TM) cells displaying an intermediate level
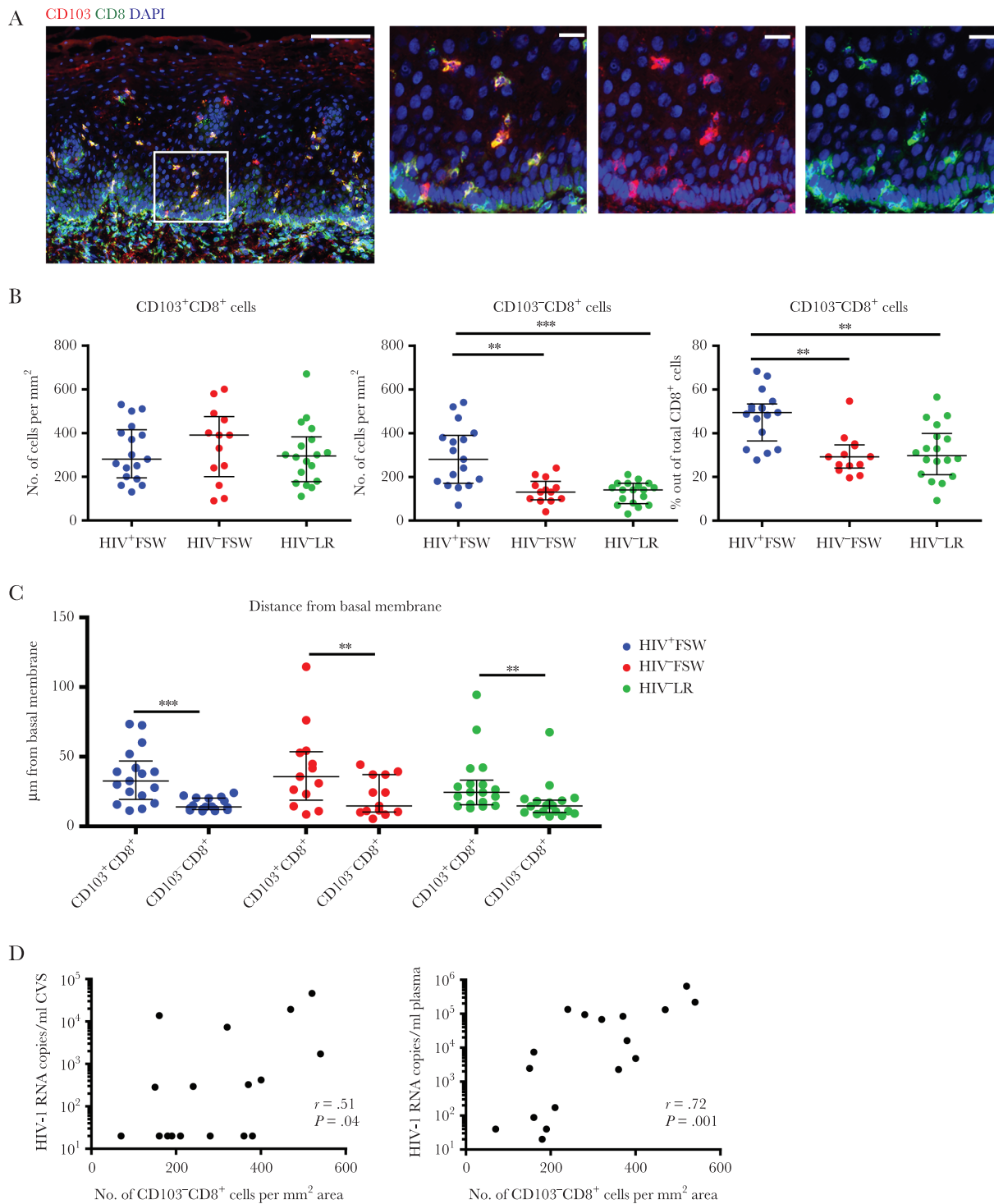
Figure 2. Visualization and enumeration of CD103+CD8+ and CD103−CD8+ cells in the ectocervical epithelium of human immunodeficiency virus (HIV)+female sex workers ([FSW] n = 17), HIV−FSW (n = 13), and HIV− lower risk nonsex working women ([HIV−LR] n = 18) groups. (a) Representative immunofluorescence images of ectocervical tissue sections, from an HIV+FSW, stained for CD103+ (red) and CD8+ (green); double-positive cells appear as yellow. 4′,6-Diamidino-2-phenylindole ([DAPI] blue) was used as a counterstain for visualization of cell nuclei. The images on the right are a magnified view of the region indicated in the box in the image to the left. The images were collected with ×20 objectives, and scale bars represent 100 μm in the image on the left and 20 μm in the images on the right. (b) Scatter plots showing numbers of CD103+CD8+ cells/mm² tissue area; CD103−CD8+ cells/mm² tissue area; percentage of CD103−CD8+ cells within total CD8+ cells in the ectocervical epithelium, quantified using the cell image analysis software CellProfiler. (c) Scatter plots showing the distribution of the median distance of CD103+CD8+ cells and CD103−CD8+ cells to the basal membrane of the ectocervical epithelium. Each circle represents a different subject: HIV+FSW (blue), HIV−FSW (red), and HIV−LR (green). Horizontal lines represent median ± interquartile range. Statistical significance was determined using the Kruskal-Wallis test, followed by Dunn's post hoc test; **, $P < .01$ and ***, $P < .001$. (d) Correlation between cervical and plasma viral load and number of CD103−CD8+ cells/mm² tissue area in the HIV+FSW group. Spearman rank correlation coefficient test was used to assess the correlation. Abbreviations: CVS, cervicovaginal secretions; RNA, ribonucleic acid.
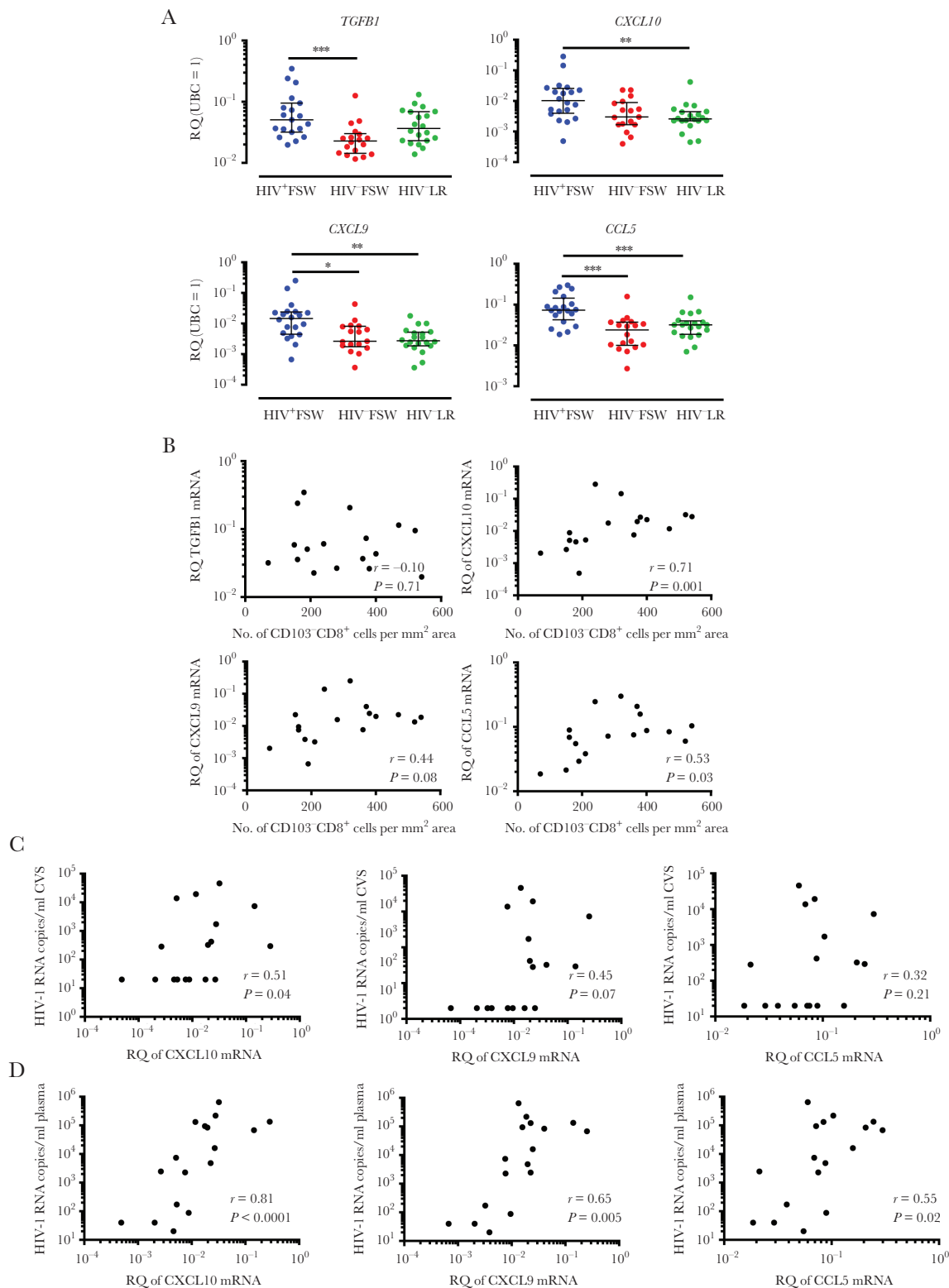
Figure 3. Messenger ribonucleic acid (mRNA) expression of cytokines and chemokines in the ectocervical tissue of human immunodeficiency virus (HIV)+female sex workers (FSW), HIV−FSW, and HIV− lower risk nonsex working women (HIV−LR) groups. (a) Scatter plots showing relative quantification (RQ) (ubiquitin C [UBC] = 1) of mRNA expression in the ectocervical tissues for *TGFB1* (HIV+FSW [n = 19], HIV−FSW [n = 18], HIV−LR [n = 20]), *CXCL10*, *CXCL9* (HIV+FSW [n = 20], HIV−FSW [n = 17], HIV−LR [n = 20]), and *CCL5* (HIV+FSW [n = 20], HIV−FSW [n = 18], HIV−LR [n = 20]). Each circle represents a different subject: HIV+FSW (blue), HIV−FSW (red), and HIV−LR (green). Horizontal lines represent median ± interquartile range. Statistical significance was determined using the Kruskal-Wallis test followed by Dunn's post hoc test; *, $P < .05$, **, $P < .01$, and ***, $P < .001$. Correlation between RQ of *TGFB1*, *CXCL10*, *CXCL9*, and *CCL5* mRNA levels, as detected by quantitative polymerase chain reaction, and the (b) number of CD103−CD8+ cells/ mm² tissue, (c) cervical viral load (VL), and (d) plasma VL in the HIV+FSW group (n = 17). Quantification of the CD103−CD8+ cells was done using the cell image analysis software, Cell Profiler. A Spearman rank correlation coefficient test was used to assess correlations.
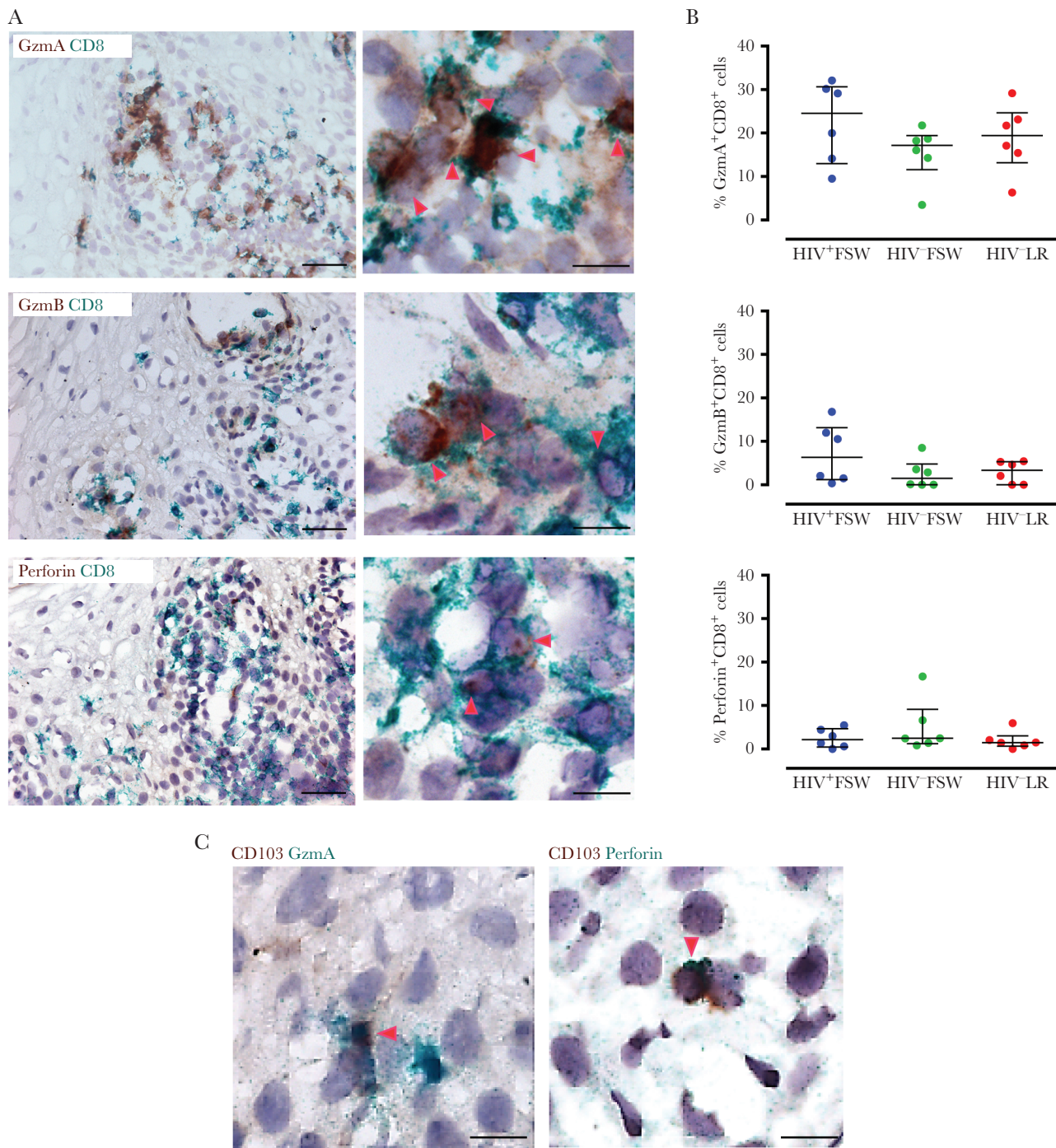
Figure 4. Expression of effector molecules in CD8^{+} and CD103^{+} cells in the ectocervical epithelium of human immunodeficiency virus (HIV)[+]female sex workers (FSW), HIV^{-}FSW, and HIV^{-} lower risk nonsex working women (HIV^{-}LR) groups. (a) Representative bright-field images of ectocervical tissue, from an HIV^{+}FSW, stained for CD8^{+} cells (green) and for granzyme (Gzm)A, GzmB, and perforin (brown). Hematoxylin staining (blue) was used as a counterstain for visualization of cell nuclei. The images were collected with ×40 and ×100 objectives; the scale bars represent 50 µm and 10 µm, respectively. (b) Scatter plots showing percentage of GzmA^{+}CD8^{+} cells, GzmB^{+}CD8^{+} cells, and perforin^{+}CD8^{+} cells within total CD8^{+} cells in the ectocervical epithelium from the HIV^{+}FSW, HIV^{-}FSW, and HIV^{-}LR groups (n = 6). Each circle represents a different subject: HIV[+]FSW (blue), HIV[-]FSW (red), and HIV[-]LR (green). Horizontal lines represent median ± interquartile range. Statistical significance was determined using the Kruskal-Wallis test followed by Dunn's post hoc test. (c) Representative bright-field images of ectocervical tissue, from an HIV^{+}FSW, stained for CD103^{+} cells (brown) and for GzmA and perforin (green). Hematoxylin staining (blue) was used as a counterstain for visualization of cell nuclei. The images were collected with ×100 objectives, and the scale bars represent 10 µm. The immunohistochemical stainings were performed on samples obtained from HIV[+]FSW, HIV[-]FSW, and HIV[-]LR groups (n = 3). The red arrows indicate double-positive cells.
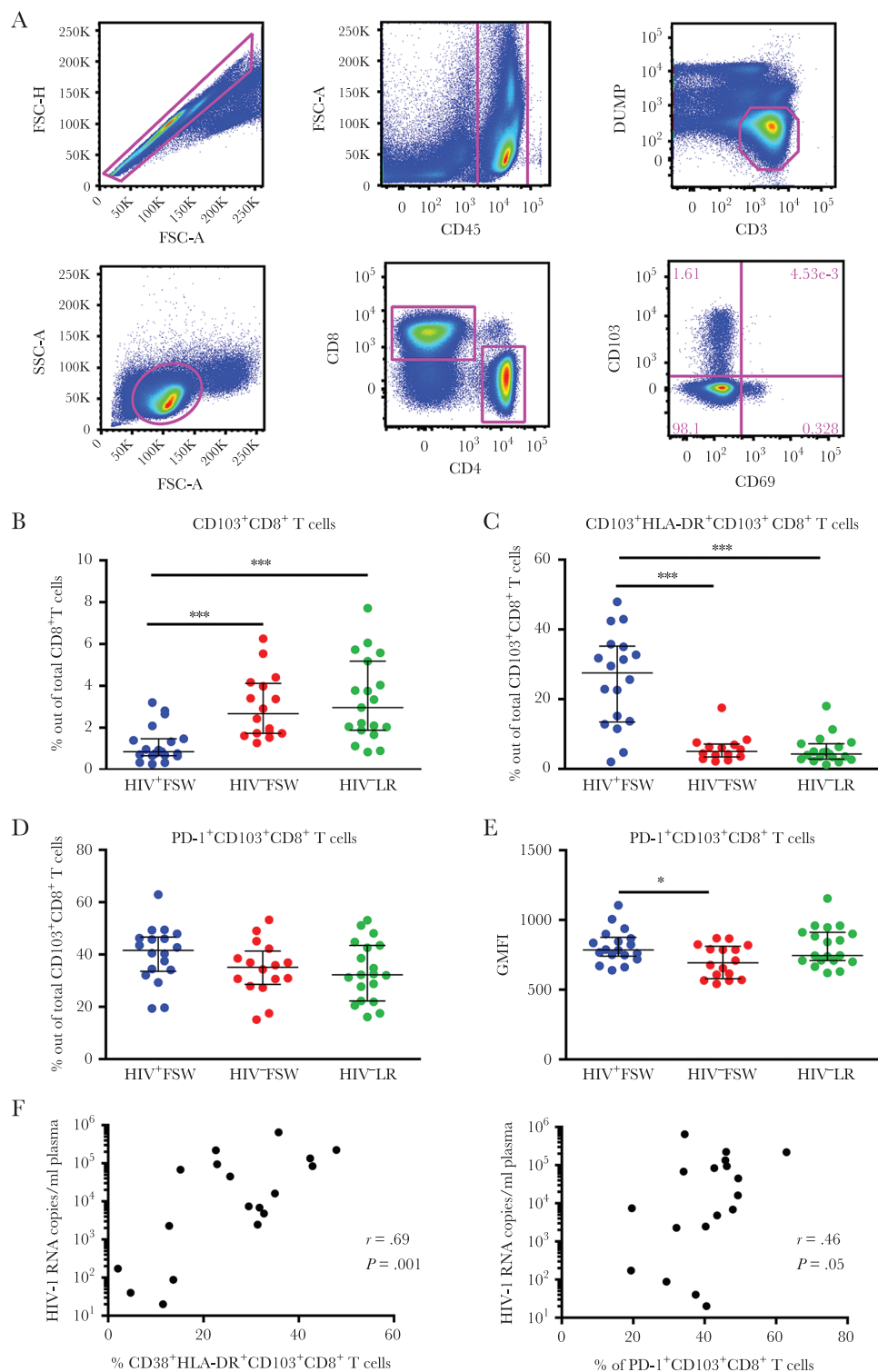
Figure 5. Comparison of the frequency and activation profile of CD103+CD8+ T cells in blood from human immunodeficiency virus (HIV)+female sex workers (FSW), HIV−FSW, and HIV− lower risk nonsex working women (HIV−LR) groups. (a) Gating strategy for circulating CD103+CD8+ T cells. Scatter plots showing (b) the proportion of CD103+CD8+ T cells within total CD8+ T cells from HIV+FSW (n = 19), HIV−FSW (n = 16), and HIV−LR (n = 19); (c) the proportion of CD38+HLA-DR+CD103+CD8+ T cells within total CD103+CD8+ T cells from HIV+FSW (n = 18), HIV−FSW (n = 14), and HIV−LR (n = 19); and (d) the proportion of PD-1+CD103+CD8+ T cells within total CD103+CD8+ T cells from HIV+FSW (n = 18), HIV−FSW (n = 16), and HIV−LR (n = 19). (e) PD-1 expression levels (geometric mean fluorescence intensity) on PD-1+CD103+CD8+ T cells from HIV+FSW (n = 18), HIV−FSW (n = 16), and HIV−LR (n = 19). Each circle represents a different subject: HIV+FSW (blue), HIV−FSW (red), and HIV−LR (green). Horizontal lines represent median ± interquartile range. Statistical significance was determined using the Kruskal-Wallis test followed by Dunn's post hoc test; *, $P < .05$ and ***, $P < .001$. (f) Correlation between plasma viral load and frequency of CD38+HLA-DR+CD103+CD8+ T cells and PD-1+CD103+CD8+ T cells in blood from the HIV+FSW group (n = 18). A Spearman rank correlation coefficient test was used to assess correlations. Abbreviations: FSC-A, forward scatter area; FSC-H, forward scatter height; RNA, ribonucleic acid; SSC-A, sidescatter area.

of differentiation (Figure 6a). Relative to the control groups, only the EM phenotype was significantly enriched within CD103$^+$CD8$^+$ T cells of the HIV$^+$FSW group (P = .0008) and correlated significantly with their corresponding plasma VL (Figure 6a and b). It is interesting to note that although CD103 expression was generally significantly lower on CD103$^+$CD8$^+$ T$_{TM}$ cells than on CD103$^+$CD8$^+$ T$_{EM}$ cells in all study groups (GMFI: TM vs EM; HIV$^+$FSW: 1647 vs 2762, P = .0002; HIV$^-$FWS: 2209 vs 3746, P = .0005; and HIV$^-$LR: 2226 vs 4579, P = .0001) (Figure 6c), the HIV$^+$FSW group had significantly lower expression of CD103 on both of these memory subsets than the control groups (P = .0001 and P = .0005, respectively) (Figure 6d).

DISCUSSION

This is the first study to characterize tissue-residency marker expression on CD8$^+$ T cells in ectocervical epithelium of healthy and HIV-infected women. We found that the majority of epithelial CD8$^+$ T cells displayed EM phenotype and expressed bona fide T$_{RM}$ markers (CD103$^+$CD69$^+$) in healthy ectocervical epithelium. Furthermore, these cells exhibited higher CD103 expression in the ectocervical epithelium, compared with submucosa, supporting the role of epithelial localization for the formation of CD103$^+$CD8$^+$ T$_{RM}$ cells [6]. Human immunodeficiency virus-specific CD8$^+$ T$_{RM}$ cells established in murine genital mucosa upon vaccination displayed significant bias in spatial localization towards epithelium, compared with submucosa [31], implying the importance of assessing T$_{RM}$ cells specifically in the epithelial compartment; the initial barrier of genital mucosa.

Several studies indicate a phenotypical heterogeneity of the T$_{RM}$ cells found in human and murine tissues, including differential CD103 expression (ie, CD103$^+$CD8$^+$ and CD103$^-$CD8$^+$ T$_{RM}$ cells) [13, 14, 16, 32], which has been furthermore associated with distinct functional capacity of these cells [16]. In this study, in agreement with previous studies, we identified both CD103$^+$CD8$^+$ and CD103$^-$CD8$^+$ T$_{RM}$ cells lodging the ectocervical epithelium. However, regardless of CD103 expression, CD8$^+$ T$_{RM}$ cells were loaded with cytotoxic granules, with no IFN-γ production observed in steady-state conditions. It is interesting to note that Posavad et al [5] reported that approximately 1.5% of cervical HSV-2-reactive CD103$^+$CD8$^+$ and CD103$^-$CD8$^+$ T cells produced IFN-γ, indicating that cervical CD8$^+$ T$_{RM}$ cells display moderate IFN-γ production capacity upon proper antigenic stimulation.

Because the epithelial mucosa is a potential entry portal and initial replication site for many STIs, including HIV, we next characterized CD8$^+$ T cells populating the ectocervical epithelium of women infected with HIV. In contrast to the healthy Swedish women, the women infected with HIV displayed an elevated frequency of CD103$^-$CD8$^+$ cells in their ectocervical epithelium. These cells were located closer to the epithelial basal membrane than the more apically located CD103$^+$CD8$^+$ cells, thus suggesting that the CD103$^-$CD8$^+$ cells and the CD103$^+$CD8$^+$ cells populate different spatial niches within the cervical epithelium. Diminished CD103 expression on CD8$^+$ cells may also be reflective of a recent influx of these cells that have not yet upregulated CD103. Nevertheless, approximately all CD8$^+$ cells were CD69$^+$, indicating that CD103$^+$CD8$^+$ cells, similar to CD103$^-$CD8$^+$ cells, belong to the T$_{RM}$ cell population.

Accumulation of epithelial CD103$^-$CD8$^+$ cells in the HIV-infected woman was unlikely due to ongoing local in situ proliferation because neither CD103$^+$ nor CD8$^+$ cells coexpressed Ki67. However, an increased number of epithelial CD103$^-$CD8$^+$ cells was associated with elevated levels of cervical CXCL10 and CXCL9 chemokines in women infected with HIV. It is notable that the chemokine receptor CXCR3 (the binding receptor for CXCL10 and CXCL9) mediated recruitment of CD8$^+$ T cells to proinflammatory microenvironments is required for differentiation of CD103$^-$CD8$^+$ T$_{RM}$ in murine gut mucosa [13]. Although TGF-β expression was also elevated in the ectocervix of HIV-infected women, it was not associated with CD103 expression on epithelial CD8$^+$ cells, similarly to what was previously observed in the cervical secretions of women infected with HIV [33]. Furthermore, interleukin-12 and type I IFN have a counteracting activity against TGF-β-reliant CD103 upregulation in mice intestine [14], indicating the impact of the overall cytokine milieu within the tissue environment.

Multiple antigen exposures and local inflammation enhance T$_{RM}$ cell recruitment to the skin in mice models [34]. Furthermore, chronic antigenic stimulation reduces CD103 upregulation on antigen-specific CD8$^+$ T cells in mice [35]. We have previously shown that the HIV-infected women included in this study had ongoing viral replication and high immune activation in their ectocervix [21, 22]. Here, we found that the number of epithelial CD103$^-$CD8$^+$ cells correlated significantly with their VL in blood and cervix and chemokine expression in ectocervix. It is thus tempting to speculate that the enhanced immune activation, including local CXCL10, CXCL9, and CCL5 chemokine expression and ongoing viral replication, is a driving force for CD103$^-$CD8$^+$ T$_{RM}$ cell recruitment and formation in the ectocervical epithelium. It is worth noting that an increased proportion of CD8$^+$ T cells expressing low levels of CD103 has been recently observed in the rectosigmoid mucosa of treatment-naive HIV-infected individuals [32]. Furthermore, these cells accounted for the majority of HIV-specific cells [32], suggesting an HIV-associated alteration of the T$_{RM}$ subset.

Epithelial CD103$^+$CD8$^+$ and CD103$^-$CD8$^+$ cells expressed cytotoxic effector molecules in all study populations. However, in lower magnitude, the expression pattern of the effector molecules seen in Kenyan woman resembled the expression observed in healthy Swedish women, namely, highest GzmA expression and nearly absent IFN-γ expression in the ectocervical epithelium. The discrepancy in the relative magnitude of expression
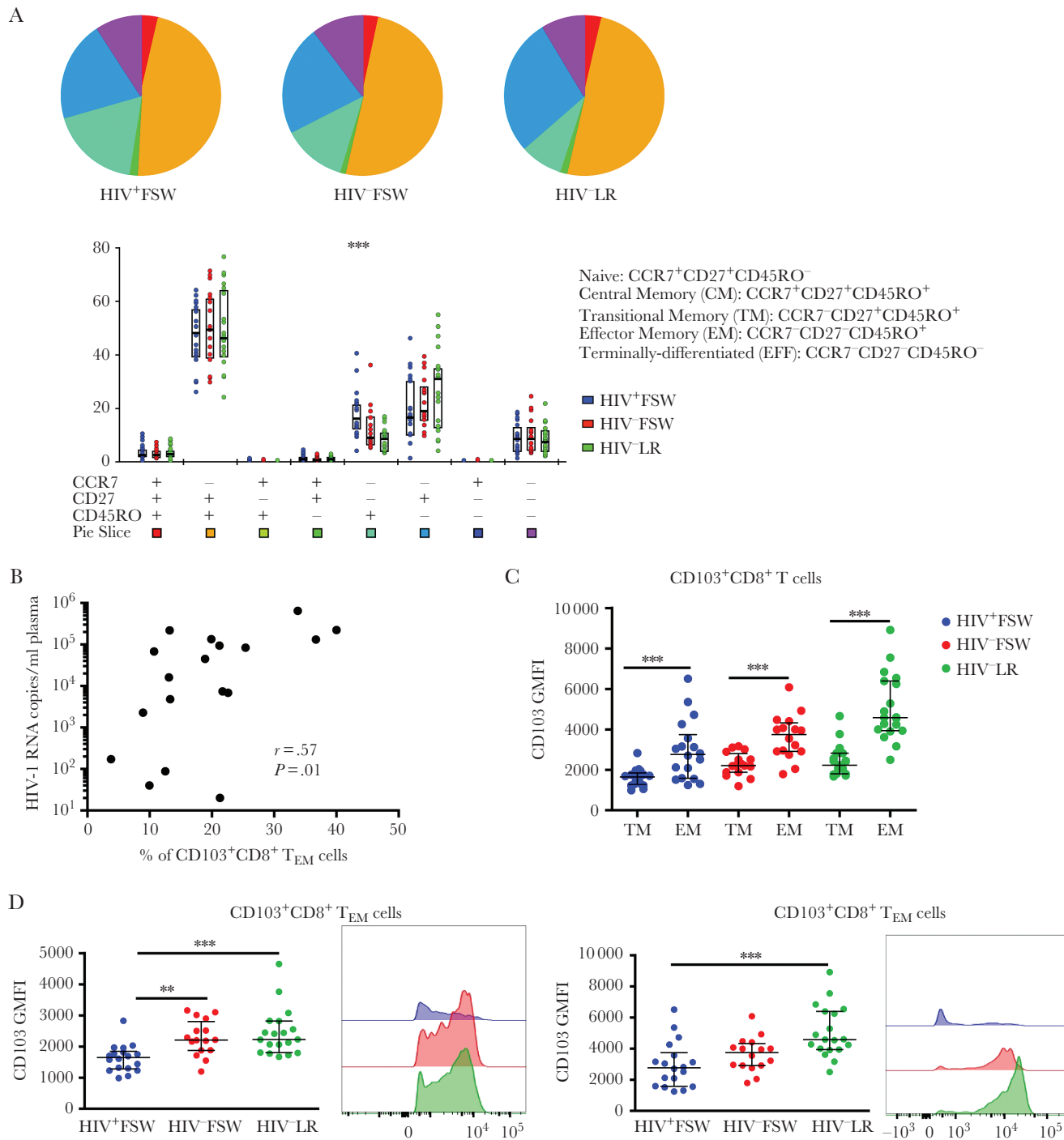
Figure 6. Characterization of the memory compartment of CD103+CD8+ T cells from blood of human immunodeficiency virus (HIV)+female sex workers (FSW) (n = 18), HIV−FSW (n = 16), and HIV− lower risk nonsex working women (HIV−LR) (n = 19) groups. (a) Pie and bar charts representing distribution of memory populations, based on CD45RO, CD27, and CCR7 expression in CD103+CD8+ T cells in the HIV+FSW (blue), HIV−FSW (red), and HIV−LR (green) groups. Statistical significance was determined using the Kruskal-Wallis test followed by Dunn's post hoc test; ***, P < .001. (b) Correlation between plasma viral load and frequency of CD103+CD8+ T_EM cells in blood from the HIV+FSW group. A Spearman rank correlation coefficient test was used to assess the correlation. (c) Scatter plot showing CD103 expression levels (geometric mean fluorescence intensity) on different memory subpopulations of CD103+CD8+ T cells, and (d) scatter plot and representative histogram showing expression levels of CD103 on CD103+CD8+ T_TM cells and CD103+CD8+ T_EM cells. Each circle represents a different subject: HIV+FSW (blue), HIV−FSW (red), and HIV−LR (green). Horizontal lines represent median ± interquartile range. Statistical significance was determined using the Kruskal-Wallis test followed by Dunn's post hoc test; **, P < .01 and ***, P < .001.

may be due to different techniques and analyzed sample types [2]. Furthermore, women infected with HIV had comparable frequencies of effector molecules expressed by epithelial CD8⁺ cells compared with the uninfected groups, similarly to what was seen in gut in HIV-infected individuals [36]. This suggests that the HIV infection does not preferentially alter the frequencies of effector CD8⁺ cells populating the ectocervical epithelium.

Antigen reactivated CD8⁺ T_{RM} cells are important for the recruitment of systemic memory cells to the site of infection [37]. In this study, we found an association between the frequencies of circulating CD103⁺CD8⁺ T cells and CD103⁺CD8⁺ cells present in the ectocervical epithelium of women infected with HIV, similarly to what was previously seen in cervical cytobrush samples from women infected with HIV [33]. Furthermore, the altered CD103 expression seen in epithelial CD8⁺ cells of women infected with HIV was also observed in their circulation. They primarily displayed lower frequencies of circulating CD103⁺CD8⁺ T cells and diminished CD103 expression on the two dominant memory cell populations. These consisted of transitional and EM, implying that CD103 expressing CD8⁺ T cells resemble antigen-experienced cells and have the capacity to recirculate between blood and peripheral nonlymphoid tissues. Within the HIV-infected group, CD103⁺CD8⁺ T cells were enriched within the EM pool, presumably reflecting an increased antigenic burden in HIV-infected individuals compared with uninfected. In addition, within the HIV-infected group, CD103⁺CD8⁺ T cells were highly activated and displayed elevated levels of PD-1 expression and thus resembled the activation/exhaustion status previously seen on the circulating CD8⁺ T cells from individuals infected with HIV [24, 29, 30, 38]. It would be interesting to further characterize the antigenic specificity of these cells as wells as their contribution to the HIV immunity.

CONCLUSIONS

In this study, we show that CD8⁺ T_{RM} cells, loaded with cytolytic molecules, are present in the ectocervical epithelium of healthy and HIV-infected women. Presence of effector CD8⁺ T cells residing at the frontline tissue barrier may have the potential to provide a robust defense against invading pathogens, and this makes these cells an attractive target for vaccination strategies approaching persistent genital infections.

Supplementary Data

Supplementary materials are available at *The Journal of Infectious Diseases* online. Consisting of data provided by the authors to benefit the reader, the posted materials are not copyedited and are the sole responsibility of the authors, so questions or comments should be addressed to the corresponding author.

Notes

References

1. Wira CR, Rodriguez-Garcia M, Patel MV. The role of sex hormones in immune protection of the female reproductive tract. Nat Rev Immunol **2015**; 15:217–30.
2. Steinert EM, Schenkel JM, Fraser KA, et al. Quantifying memory CD8 T cells reveals regionalization of immunosurveillance. Cell **2015**; 161:737–49.
3. Thome JJ, Yudanin N, Ohmura Y, et al. Spatial map of human T cell compartmentalization and maintenance over decades of life. Cell **2014**; 159:814–28.
4. Moylan DC, Goepfert PA, Kempf MC, et al. Diminished CD103 (αEβ7) expression on resident T cells from the female genital tract of HIV-positive women. Pathog Immun **2016**; 1:371–87.
5. Posavad CM, Zhao L, Dong L, et al. Enrichment of herpes simplex virus type 2 (HSV-2) reactive mucosal T cells in the human female genital tract. Mucosal Immunol **2017**; 10:1259–69.
6. Mackay LK, Rahimpour A, Ma JZ, et al. The developmental pathway for CD103(+)CD8+ tissue-resident memory T cells of skin. Nat Immunol **2013**; 14:1294–301.
7. Sheridan BS, Pham QM, Lee YT, Cauley LS, Puddington L, Lefrançois L. Oral infection drives a distinct population of intestinal resident memory CD8(+) T cells with enhanced protective function. Immunity **2014**; 40:747–57.
8. Shin H, Iwasaki A. A vaccine strategy that protects against genital herpes by establishing local memory T cells. Nature **2012**; 491:463–7.
9. Zhang N, Bevan MJ. Transforming growth factor-β signaling controls the formation and maintenance of gut-resident memory T cells by regulating migration and retention. Immunity **2013**; 39:687–96.

10. Iijima N, Iwasaki A. T cell memory. A local macrophage chemokine network sustains protective tissue-resident memory CD4 T cells. Science **2014**; 346:93–8.

11. Cepek KL, Shaw SK, Parker CM, et al. Adhesion between epithelial cells and T lymphocytes mediated by E-cadherin and the alpha E beta 7 integrin. Nature **1994**; 372:190–3.

12. Skon CN, Lee JY, Anderson KG, Masopust D, Hogquist KA, Jameson SC. Transcriptional downregulation of S1pr1 is required for the establishment of resident memory CD8+ T cells. Nat Immunol **2013**; 14:1285–93.

13. Bergsbaken T, Bevan MJ. Proinflammatory microenvironments within the intestine regulate the differentiation of tissue-resident CD8+ T cells responding to infection. Nat Immunol **2015**; 16:406–14.

14. Bergsbaken T, Bevan MJ, Fink PJ. Local inflammatory cues regulate differentiation and persistence of CD8+ tissue-resident memory T cells. Cell Rep **2017**; 19:114–24.

15. Mackay LK, Wynne-Jones E, Freestone D, et al. T-box transcription factors combine with the cytokines TGF-β and IL-15 to control tissue-resident memory T cell fate. Immunity **2015**; 43:1101–11.

16. Watanabe R, Gehad A, Yang C, et al. Human skin is protected by four functionally and phenotypically discrete populations of resident and recirculating memory T cells. Sci Transl Med **2015**; 7:279ra39.

17. Çuburu N, Wang K, Goodman KN, et al. Topical herpes simplex virus 2 (HSV-2) vaccination with human papillomavirus vectors expressing gB/gD ectodomains induces genital-tissue-resident memory CD8+ T cells and reduces genital disease and viral shedding after HSV-2 challenge. J Virol **2015**; 89:83–96.

18. Maldonado L, Teague JE, Morrow MP, et al. Intramuscular therapeutic vaccination targeting HPV16 induces T cell responses that localize in mucosal lesions. Sci Transl Med **2014**; 6:221ra13.

19. Cheuk S, Schlums H, Gallais Sérézal I, et al. CD49a expression defines tissue-resident CD8+ T cells poised for cytotoxic function in human skin. Immunity **2017**; 46:287–300.

20. Cheuk S, Wikén M, Blomqvist L, et al. Epidermal Th22 and Tc17 cells form a localized disease memory in clinically healed psoriasis. J Immunol **2014**; 192:3111–20.

21. Gibbs A, Hirbod T, Li Q, et al. Presence of CD8+ T cells in the ectocervical mucosa correlates with genital viral shedding in HIV-infected women despite a low prevalence of HIV RNA-expressing cells in the tissue. J Immunol **2014**; 192:3947–57.

22. Hirbod T, Kimani J, Tjernlund A, et al. Stable CD4 expression and local immune activation in the ectocervical mucosa of HIV-infected women. J Immunol **2013**; 191:3948–54.

23. Hasselrot K, Cheruiyot J, Kimani J, Ball TB, Kaul R, Hirbod T. Feasibility and safety of cervical biopsy sampling for mucosal immune studies in female sex workers from Nairobi, Kenya. PLoS One **2012**; 7:e47570.

24. Buggert M, Frederiksen J, Noyan K, et al. Multiparametric bioinformatics distinguish the CD4/CD8 ratio as a suitable laboratory predictor of combined T cell pathogenesis in HIV infection. J Immunol **2014**; 192:2099–108.

25. Carpenter AE, Jones TR, Lamprecht MR, et al. CellProfiler: image analysis software for identifying and quantifying cell phenotypes. Genome Biol **2006**; 7:R100.

26. Kamentsky L, Jones TR, Fraser A, et al. Improved structure, function and compatibility for CellProfiler: modular high-throughput image analysis software. Bioinformatics **2011**; 27:1179–80.

27. Brismar Wendel S, Kaldensjö T, Peterson P, Andersson S, Broliden K, Hirbod T. Slumbering mucosal immune response in the cervix of human papillomavirus DNA-positive and -negative women. Int J Oncol **2010**; 37:1565–73.

28. Livak KJ, Schmittgen TD. Analysis of relative gene expression data using real-time quantitative PCR and the 2(-Delta Delta C(T)) method. Methods **2001**; 25:402–8.

29. Day CL, Kaufmann DE, Kiepiela P, et al. PD-1 expression on HIV-specific T cells is associated with T-cell exhaustion and disease progression. Nature **2006**; 443:350–4.

30. Petrovas C, Casazza JP, Brenchley JM, et al. PD-1 is a regulator of virus-specific CD8+ T cell survival in HIV infection. J Exp Med **2006**; 203:2281–92.

31. Tan HX, Wheatley AK, Esterbauer R, et al. Induction of vaginal-resident HIV-specific CD8 T cells with mucosal prime-boost immunization. Mucosal Immunol **2017**; doi:10.1038/mi.2017.89.

32. Kiniry BE, Li S, Ganesh A, et al. Detection of HIV-1-specific gastrointestinal tissue resident CD8+ T-cells in chronic infection. Mucosal Immunol **2017**; doi:10.1038/mi.2017.96.

33. Kiravu A, Gumbi P, Mkhize NN, Olivier A, Denny L, Passmore JA. Evaluation of CD103 (αEβ7) integrin expression by CD8 T cells in blood as a surrogate marker to predict cervical T cell responses in the female genital tract during HIV infection. Clin Immunol **2011**; 141:143–51.

34. Davies B, Prier JE, Jones CM, Gebhardt T, Carbone FR, Mackay LK. Cutting edge: tissue-resident memory T cells generated by multiple immunizations or localized deposition provide enhanced immunity. J Immunol **2017**; 198:2233–7.

35. Casey KA, Fraser KA, Schenkel JM, et al. Antigen-independent differentiation and maintenance of effector-like resident memory T cells in tissues. J Immunol **2012**; 188:4866–75.

36. Kiniry BE, Ganesh A, Critchfield JW, et al. Predominance of weakly cytotoxic, T-betLowEomesNeg CD8+ T-cells in human gastrointestinal mucosa: implications for HIV infection. Mucosal Immunol **2017**; 10:1008–20.

37. Schenkel JM, Fraser KA, Vezys V, Masopust D. Sensing and alarm function of resident memory CD8+ T cells. Nat Immunol **2013**; 14:509–13.

38. Giorgi JV, Detels R. T-cell subset alterations in HIV-infected homosexual men: NIAID Multicenter AIDS cohort study. Clin Immunol Immunopathol **1989**; 52:10–8.